JOURNAL OF THERMOPHYSICS AND HEAT TRANSFER
Vol. 17, No. 2, April–June 2003

Technical Notes

TECHNICAL NOTES are short manuscripts describing new developments or important results of a preliminary nature. These Notes cannot exceed six manuscript pages and three figures; a page of text may be substituted for a figure and vice versa. After informal review by the editors, they may be published within a few months of the date of receipt. Style requirements are the same as for regular contributions (see inside back cover).

Temperature Distribution in a Porous Medium with Solar Incidence and Downward Flow

Pai-Chuan Liu*
Chinese Military Academy,
Fengshang 830, Taiwan, Republic of China

Nomenclature

C_p = specific heat at constant pressure, J/kg-K
g = acceleration of gravity, m/s^2
I_{in} = incident radiative intensity, W/m^2-steradian
I_{tr} = transmitted radiative intensity, W/m^2-steradian
k = thermal conductivity, W/m-K
L = fluid layer thickness, m
Pe = Peclet number, $w_0 L/\alpha_m$
q_r = rate of heat generation by absorption, W/m^3
R^* = ratio of internal and external Rayleigh number, Ra_i/Ra_e
Ra_e = external Rayleigh number, $g\beta(T_1 - T_2)L^3/(\alpha_m \upsilon_f)$
Ra_i = internal Rayleigh number, $g\beta I_{\text{tr}} L^4/(\kappa_m \alpha_m \upsilon_f)$
r = bounding surface reflectivity
T = temperature, K
T^* = nondimensional temperature gradient, $(T - T_2)/(T_1 - T_2)$
w_0 = downward fluid flow velocity, m/s
x = Cartesian coordinate, m
Z = nondimensional thickness, z/L
z = Cartesian coordinate, m
α_m = effective thermal diffusivity, $k_m/(\rho C_p)_f$
β = thermal expansion coefficient, K^{-1}
κ = extinction coefficient, m^{-1}
ρ = fluid density, kg/m^3
τ = optical thickness, κL
τ_{eff} = effective transmissivity
υ = kinematic viscosity, m^2/s

Subscripts

f = fluid properties
m = fluid-saturated porous medium properties
1 = lower boundary
2 = upper boundary

Introduction

FLUID flow through a porous medium is a subject of interest because many engineering applications utilize porous media, for example, heat exchangers, solar-energy collection systems, chemical reactors, heat pipes, and electronic cooling devices. Thus, the investigation of convective heat transfer in a porous medium has received a great deal of attention in the past three decades. Knowledge of the temperature distribution in a fluid-saturated porous medium is important in the study of natural convection. In particular, it plays a significant role in the investigation of saltless solar-pond design as indicated by Hadim and Burmeister.[1] A saltless solar pond consists of continuously injecting cool make-up water from the top, while warm water is withdrawn from the bottom surface for distribution. Thus, a gentle downward flow of water is created in the direction of increasing temperature gradient. Hadim and Burmeister[1] stated that solar-pond efficiency could be increased because downward convection of stored energy in the water near the bottom is greater than the conduction through the water at the top. Smiley and Burmeister[2] have verified that the amount of useful heat collected in a downward-convecting solar pond could be 35% higher as compared to the conventional stagnant salt-gradient solar pond. The study also revealed that the downward convective velocity must be small, on the order of 10^{-3} m/h, in order to achieve usefully high bottom temperatures in a downward-convecting solar pond. Moreover, a porous medium was introduced into the solar-pond design in order to overcome the upward natural convection present without the medium. Therefore, the stability criteria pertinent to this physical situation are needed to study the efficiency of the proposed downward-convecting solar-pond design. The steady-state temperature distribution within a solar pond is known a priori for the determination of the needed stability criteria.[1]

The stability of a horizontal fluid-saturated porous medium with externally imposed downward convection and distributed internal heat generation was first considered by Hadim and Burmeister.[1] The boundaries confining the fluid are assumed to be at prescribed temperatures with reflections from the top and bottom of the pond neglected in the analysis. It is understood there are numerous factors that affect the initiation of convective flow patterns in the fluid. Therefore, there is a strong possibility that with this oversimplification the temperature distribution and stability criteria calculations are erroneous. The influence of surface reflection in fluid stability has been studied by Liu.[3,4] The experience demonstrates that this could significantly alter the uncertainty in the solar-pond performance.

In the present study the energy equation governs an infinite horizontal layer of fluid filled with a saturated porous medium confined between two isothermal plates subjected to external radiative incidence. The imposed downward-convection problem is analytically solved to determine the temperature distribution. The parameters that control the temperature profile include the internal and external Rayleigh numbers, Peclet number, optical thickness, and surface reflectivities. The primary objective of this investigation is to determine the influence of these parameters on the temperature distribution. Furthermore, the implications regarding fluid stability criteria will be addressed. These results are applicable to the conceptual design and operation of a solar pond. The phenomena described in this study are typical of various chemical processes, fluidized beds, and oceanographic and other engineering applications.

Problem Formulation and Solution

The geometry for the physical problem is shown in Fig. 1. It depicts an incompressible fluid-saturated porous layer of infinite horizontal extent, which is confined to the region $0 \le z \le L$. The top surface of the layer is subjected to incident solar radiation and a steady downward flow. Both the upper and lower rigid boundaries

Received 27 August 2001; revision received 4 November 2002; accepted for publication 29 December 2002.

*Associate Professor, Department of Mathematics; pcliu@cc.cma.edu.tw.

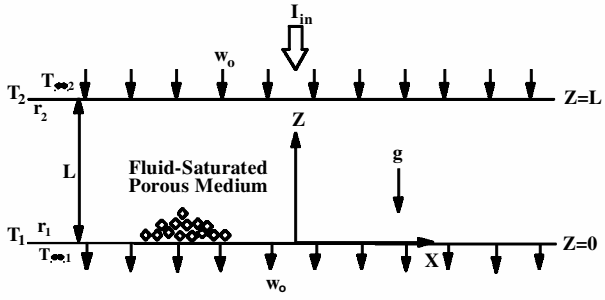

Fig. 1 Schematic diagram of the physical problem.

exchange heat with the environment, which is maintained at a constant temperature. The z axis is taken as the vertical coordinate with the origin at the bottom rigid surface, and the x axis is the horizontal coordinate (along the bottom solid surface). The liquid is heated by a nonuniform volumetric energy source of strength q^r, as a result of external radiation incident on the upper boundary.

It is assumed that all fluid properties, such as viscosity, thermal conductivity, specific heat, and thermal expansion coefficient, are constant and independent of temperature. In this study the aim is to investigate the effects of the incident radiative source I_{in}, the thermal boundary condition (Biot number), internal and external Rayleigh numbers, Peclet number, optical thickness, and surface reflectivities on the temperature distribution that influence the stability conditions of the horizontal liquid layer. The derivation of the steady-state temperature of the fluid layer is presented and discussed next.

The equation governing the steady-state temperature across the liquid layer is given by[1]

$$\frac{\mathrm{d}^2T}{\mathrm{d}z^2} + \frac{w_0}{\alpha_m}\frac{\mathrm{d}T}{\mathrm{d}z} + \frac{1}{k_m}\frac{\mathrm{d}q_r}{\mathrm{d}z} = 0 \tag{1}$$

It is assumed that the temperature is uniform and constant throughout the boundary. The temperatures of the lower and upper boundary surfaces are designated as T_1 and T_2, respectively. Thermal radiation with intensity I_{in} is incident normal to the upper surface. The liquid layer is assumed to be an absorbing and nonscattering medium in which emission is negligible. The reflectivities at the lower and upper surfaces are r_1 and r_2, respectively. The portion of the incident thermal radiative intensity that has penetrated and been transmitted into the fluid layer is

$$I_{\text{tr}} = I_{\text{in}}\tau_{\text{eff}} \tag{2}$$

Thus, the amount of incident thermal radiation that has penetrated to a depth $(L\text{-}z)$ can be written as[5,6]

$$\frac{\mathrm{d}q_r}{\mathrm{d}z} = \frac{I_{\text{tr}}\kappa[\exp(\kappa z) + r_1\exp(-\kappa z)]}{\exp(\kappa L) - r_1r_2\exp(-\kappa L)} \tag{3}$$

The volumetric rate of heat generation $\mathrm{d}q_r/\mathrm{d}z$ therefore refers to the incident thermal radiation that penetrated into and is absorbed in the fluid body. By incorporating the rate of volumetric heat generation in the governing energy Eq. (1), one can solve for the steady-state temperature profile of the conduction regime from

$$\frac{\mathrm{d}^2T}{\mathrm{d}z^2} + \frac{w_0}{\alpha_m}\frac{\mathrm{d}T}{\mathrm{d}z} + \frac{1}{k_m}\frac{I_{\text{th}}\kappa[\exp(\kappa z) + r_1\exp(-\kappa z)]}{\exp(\kappa L) - r_1r_2\exp(-\kappa z)]} = 0 \tag{4}$$

subject to the boundary conditions

$$T|_{z=0} = T_1 \tag{5}$$

$$T|_{z=L} = T_2 \tag{6}$$

The solution of the preceding system can be obtained, and the dimensionless steady-state temperature distribution across the fluid layer takes the form

$$T^* = \frac{T - T_2}{T_1 - T_2} = 1 + \frac{R^*}{\left(e^{\tau} - r_1r_2e^{-\tau}\right)}\left[\frac{r_1(1 - e^{-\tau Z})}{(\tau - Pe)} + \frac{1 - e^{\tau Z}}{(\tau + Pe)}\right]$$
$$- \frac{R^*(1 - e^{-PeZ})}{\left(e^{\tau} - r_1r_2e^{-\tau}\right)(1 - e^{-Pe})}\left[\frac{r_1(1 - e^{-\tau})}{(\tau - Pe)} + \frac{1 - e^{\tau}}{(\tau + Pe)}\right]$$
$$- \frac{1 - e^{-PeZ}}{1 - e^{-Pe}} \tag{7}$$

The nondimensional numbers in Eq. (7) are

$$P_e = (w_0/\alpha_m)L, \qquad \tau = \kappa L, \qquad R^* = Ra_i/Ra_e$$

For the limiting case of no downward flow ($w_0 = 0$) and external thermal radiation incident at the upper boundary ($I_{\text{tr}} = 0$), Eq. (7) reduces to

$$T^* = 1 - Z \tag{8}$$

which represents a standard linearly decreasing temperature distribution across the fluid layer without the effect of the external heat source, which agrees with the results by Sparrow et al.[7]

Results and Discussion

The aim of this study is to investigate the effect of the incident radiative source on natural convection in a horizontal liquid layer. As a result of the absorbed thermal radiative energy, the base-state temperature gradient plays an important role regarding the conditions leading to the onset of convective motion. The onset of convective motion is strongly dependent on the Peclet number, internal and external Rayleigh numbers, optical thickness, and surface reflectivities.

As mentioned before, the nonuniformity in the steady-state conduction temperature gradient across the liquid layer is caused by the absorption of external thermal irradiation. The effects of thermal irradiation can be explained by referring to the steady-state temperature gradient across the liquid layer, as shown in Fig. 2. The steady-state dimensionless temperature gradients T^* are presented for various values of the internal and external Rayleigh number ratios ($R^* = Ra_i/Ra_e$) for $\tau = 0.2$, $Pe = 1$, $r_1 = 0.5$, and $r_2 = 0.5$. The internal and external Rayleigh numbers are indicators of the thermal irradiation strength and the viscous force, respectively. If $R^* = 0$, T^* is the standard linearly decreasing temperature distribution across a fluid layer without the effect of an external heat source. In other words, the deviation of T^* from the standard linear decreasing function is a measure of the nonlinearity of the temperature distribution induced by the external heat source. The influence of the incident energy on the temperature gradient has a profound effect as Ra_i increases. As the external energy incident at the upper boundary increases and as most of the incoming energy is absorbed in the upper stratum, the temperature gradient is increased drastically in the upper half of the liquid layer. The temperature distribution trend reverses around the midpoint of the fluid layer because the dominance

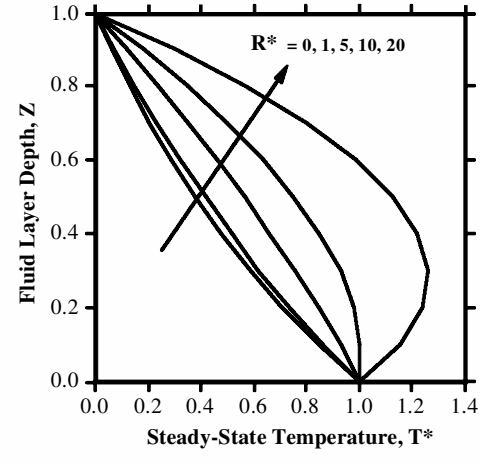

Fig. 2 Influence of viscous force on steady-state temperature distribution with $\tau = 0.2$, $Pe = 1$, $r_1 = 0.5$, and $r_2 = 0.5$.

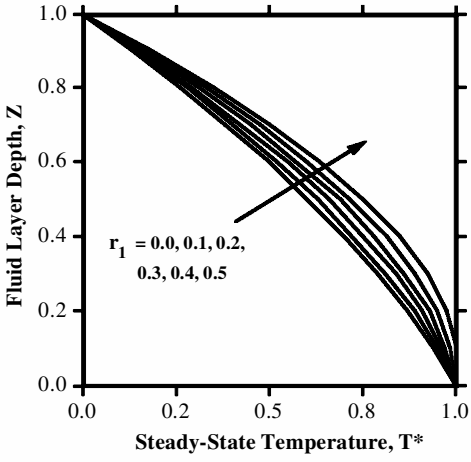

Fig. 3a Influence of lower boundary reflectivity on steady-state temperature distribution with $\tau = 0.2$, $Pe = 1$, $r_2 = 0.5$, and $R^* = 10$.

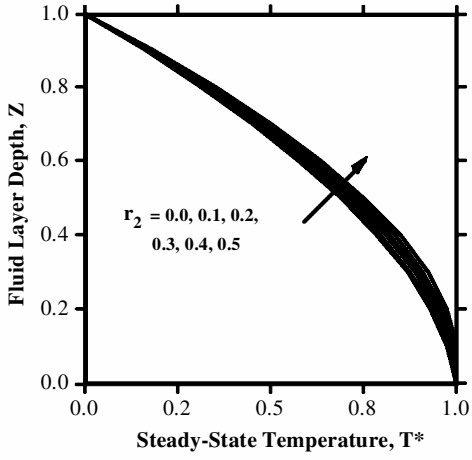

Fig. 3b Influence of upper boundary reflectivity on steady-state temperature distribution with $\tau = 0.2$, $Pe = 1$, $r_1 = 0.5$, and $R^* = 10$.

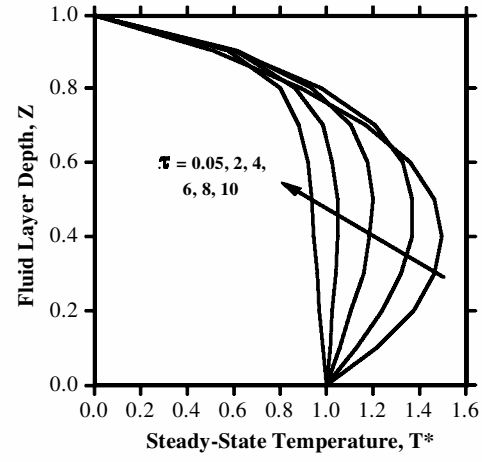

Fig. 4 Influence of absorption on steady-state temperature distribution with $Pe = 1$, $r_1 = 0.5$, $r_2 = 0.5$, and $R^* = 10$.

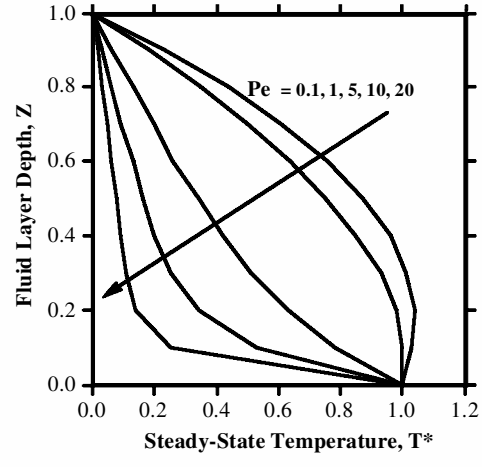

Fig. 5 Influence of downward flow on steady-state temperature distribution with $\tau = 0.2$, $r_1 = 0.5$, $r_2 = 0.5$, and $R^* = 10$.

of the viscous effect will eventually overcome the heating effect of the external heat source. The temperature profile should therefore first increase and then decrease as shown in Fig. 2, which is almost parabolic in nature when plotted as a function of the nondimensionless liquid thickness. A destabilizing nonlinear temperature gradient occurs near the midpoint of the fluid layer, and the system becomes more unstable as the thermal irradiation strength increases.

The relative effect of the boundary reflectivities is shown in Figs. 3a and 3b. In general, the base-state temperature profile has the steepest slope when both boundaries are perfectly reflecting surfaces. In this case the thermal energy is reflected and retained within the fluid layer. Thus, the maximum amount of energy is stored within the fluid layer that results in a large temperature gradient across the fluid. As a consequence, this produces the least stable system when $r_1 = r_2 = 1$. The reflectance for most substances used in solar ponds is less than 0.5 for most engineering applications. To that effect, the maximum reflectances for both boundaries are limited to 0.5 or less throughout this study. As the incoming energy is reflected at both boundaries, the temperature profile exhibits a slightly higher value at the lower half or near the bottom of the fluid layer as a result of the mixing effect of the downward fluid flow at the upper boundary.

The influence of the optical thickness on the base-state temperature profile is shown in Fig. 4. Note that the optical thickness τ is defined as the product of the absorption coefficient κ and the thickness of the liquid layer L for a nonscattering medium. For small optical thicknesses the incoming energy is absorbed uniformly throughout the fluid layer. The temperature gradient corresponds to the case of uniform heat generation and deviates from unity with a smooth slope. However, the influence of the optical thickness on the temperature gradient has a more profound effect as it approaches the optically thick limit. As $\tau \gg 1$, most of the radiative energy is absorbed in the upper strata. As a result, the temperature gradient is steep near the upper boundary of the liquid layer. The upper stratum is less stable than the lower region that has a more uniform temperature.

The Peclet number is a measure of the flow strength of the externally imposed downward velocity w_0. As the downward velocity decreases, the fluid system will become less stable as a result of the slower fluid movement (reduction in mixing effect). Therefore the nondimensional steady-state temperature distribution will increase as the Peclet number decreases. As the downward velocity of the external fluid increases, it does not provide sufficient time for the incoming external thermal energy to heat up only a certain portion of the fluid layer to induce fluid instability as a result of the continuous mixing effect. The effect of the Peclet number is shown in Fig. 5.

Conclusion

The temperature distributions within a fluid-saturated porous medium confined between two parallel layers subjected to external thermal irradiation while both surfaces are maintained at constant boundary temperature were presented. The parameters that control the temperature distribution, including the Peclet number, optical thickness, surface reflectivities, and internal and external Rayleigh numbers, were all examined in detail. The temperature distribution is almost parabolic in nature when plotted as a function of the nondimensional location within the fluid layer and reduces to the standard linear curve when the preceding influential factors were absent from the porous fluid layer. The increase of energy absorption, surface reflectivities, and external incident energy increase the

nonlinearity of the temperature distribution. An exception to this trend occurs for increasing the externally imposed downward make-up water. The rationale is that less energy will be accumulated and retained within the system as the water velocity increases, which causes less thermal disturbance in the fluid layer. As external energy is accumulated within the fluid, the temperature rises, and the location of the maximum temperature lies near the center or the lower portion of the fluid layer. The results presented in this study should provide useful information for actual stability computation in applications such as solar pond and industrial fluidized bed designs.

References

[1]Hadim, A., and Burmeister, L. C., "Onset of Convection in a Porous Medium with Internal Heat Generation and Downward Flow," *Journal of Thermophysics and Heat Transfer*, Vol. 2, No. 4, 1988, pp. 343–351.

[2]Smiley, J. A., and Burmeister, L. C., "Potential Improvement of Solar Pond Efficiency by Downward Convection," American Society of Mechanical Engineers, Paper 77-WA/HT-6, 1977.

[3]Liu, P.-C., "Thermocapillary Instability in a Horizontal Liquid Layer Subjected to a Transverse Magnetic Field and Irradiation," *International Communications in Heat and Mass Transfer*, Vol. 22, No. 5, 1995, pp. 649–660.

[4]Liu, P.-C., "Onset of Benard-Marangoni Convection in a Rotating Liquid Layer with Nonuniform Volumetric Energy Sources," *International Journal of Heat and Fluid Flow*, Vol. 17, No. 6, 1996, pp. 579–586.

[5]Yucel, A., and Bayazitoglu, Y., "Onset of Convection in Fluid Layers with Non-Uniform Volumetric Energy Sources," *Journal of Heat Transfer*, Vol. 101, No. 3, 1979, pp. 666–671.

[6]Lam, T. T., and Bayazitoglu, Y., "Marangoni Instability with Non-Uniform Volumetric Energy Sources Due to Incident Radiation," *Acta Astronautica*, Vol. 17, No. 1, 1988, pp. 31–38.

[7]Sparrow, E. M., Goldstein, R. J., and Jonsson, V. K., "Thermal Instability in a Horizontal Fluid Layer: Effect of Boundary Conditions and Non-Linear Temperature Profile," *Journal of Fluid Mechanics*, Vol. 18, No. 1, 1964, pp. 513–528.

Heat Transport Augmentation in Rayleigh–Bénard Cells Containing Two Pure Gases Mixtures

Mohammad M. Papari*
Shiraz University, 71454 Shiraz, Iran
and
Antonio Campo†
University of Vermont, Burlington, Vermont 05405

Introduction

AN IMPORTANT subclass of natural heat convection problems deals with confined flows that are induced inside stationary cavities when a temperature differential is prescribed at two opposing walls. In general, when natural convection occurs in closed spaces, heat transfer enhancement becomes difficult because of the low fluid velocities that are generated by gravitational flows. Therefore, it is of fundamental and practical interest to explore passive instruments that are conducive to the augmentation of heat in cavities. This Note presents a study of a Rayleigh–Bénard (RB) cell to investigate the heat transfer capabilities of various mixtures of pure gases that may be used as cooling media. A search of the specialized literature reveals that papers on the heat transfer enhancement in a gas-filled RB cell have not been published.

Heat Transport in an RB Cell

An RB cell is defined as an enclosed space long and wide in the horizontal direction. The RB cell is bounded by two large horizontal walls, the lower wall is held at a high temperature T_h and the upper wall at a low temperature T_c. The cell contains a coolant, which may be a single-phase liquid or gas.

The physics of fluids stipulates that the heat transport by natural convection in an RB cell is conformed by two modes. The first mode is prototypical of molecular conduction of heat in the layer of quiescent fluid. In this mode, the buoyant forces are weak and unable to overcome the viscous forces creating a force imbalance. Thus, the transfer of heat across the fluid layer is portrayed by a Nusselt number equal to one, $Nu_\delta = 1$. This plain pattern persists unaltered with increasing values of the Rayleigh number, up to a critical Rayleigh number $Ra_{\delta,\mathrm{crit}}$ in the vicinity of 1708. When the temperature differential, $T_h - T_c$, is gradually increased, the buoyancy forces are intensified, and eventually the buoyancy forces outweigh the viscous forces. This state of affairs is governed by $Ra_\delta > Ra_{\delta,\mathrm{crit}}$, and the fluid circulation becomes stronger. The fluid movement, coupled with molecular heat conduction, brings a second mode of heat transport, that is, natural convection. This situation is connected to moderate-to-large values of Rayleigh numbers Ra_δ in the range $1708 < Ra_\delta < 3.2 \times 10^5$. Within this Rayleigh number Ra_δ interval, the fluid possesses laminar motion and takes the form of two-dimensional regularly spaced counter-rotating roll cells of square cross section. These roll cells are traditionally recognized as Bénard cells.[1] Further increases in the temperature difference, $T_h - T_c$, exceed the upper limit of $Ra_\delta = 3.2 \times 10^5$, carrying with it two-dimensional roll cells that break apart and immediately form three-dimensional cells that appear hexagonal in shape when viewed from above. At $Ra_\delta \gg 3.2 \times 10^5$, the natural convective flow energizes even further, the number of cells multiply and become narrower, and the flow becomes turbulent and oscillatory. Eventually, the three-dimensional cell structures disappear.

The rate of heat transport Q in an RB cell is calculated from Newton's law of cooling:

$$Q = hA(T_h - T_c) \tag{1}$$

where h is the heat transfer coefficient, A is the area of a horizontal wall, and $T_h - T_c$ is the temperature difference impressed by the opposing horizontal walls. For the estimation of h, Jakob[2] developed the first experimental-based correlation equation:

$$Nu_\delta = CRa_\delta^n \tag{2}$$

where

$$Nu_\delta = h\delta/\lambda, \qquad Ra_\delta = g\beta\left(\rho^2 C_p/\eta\lambda\right)(T_h - T_c)\delta^3 \tag{3}$$

Equation (2) covers all gases contained in the Prandtl number band $0.5 \le Pr \le 2$. The thermophysical properties of the gases are evaluated at a film temperature $T_{\mathrm{av}} = (T_h + T_c)/2$.

Levels of Heat Transport Imparted by a Mixture of Two Pure Gases

At subcritical Rayleigh numbers, $Ra_\delta < 1708$, the mode of molecular conduction of heat in an RB cell predominates; this mode is susceptible to only one thermophysical property, that is, the thermal conductivity λ. Consequently, the sole way for enhancing the heat transport in this reduced Rayleigh number Ra_δ subinterval is to choose a gas having a high thermal conductivity λ, for instance, helium (He) or hydrogen (H_2).

Conversely, for supercritical Rayleigh numbers, $Ra_\delta > 1708$, the thermal buoyancy forces in the gas-filled RB cell are stimulated, and a fluid motion confined by the horizontal walls is induced. Under these circumstances, the objective is to invigorate the mode by natural convection (molecular heat conduction and fluid motion) by

Received 25 February 2002; revision received 8 December 2002; accepted for publication 9 December 2002.

*Assistant Professor, College of Science, Department of Chemistry.
†Associate Professor, Department of Mechanical Engineering. Member AIAA.